Simulation Analysis of Key Component Structure Optimization of Corn Mixed Flow Drying Device

Siyu Chen, Rui Qiao, Tian Yu, Wanxin Song, and Chunshan Liu *

* *Corresponding author: liuchunshan_2001@163.com*

DOI: 10.15376/biores.20.2.3085-3100

GRAPHICAL ABSTRACT

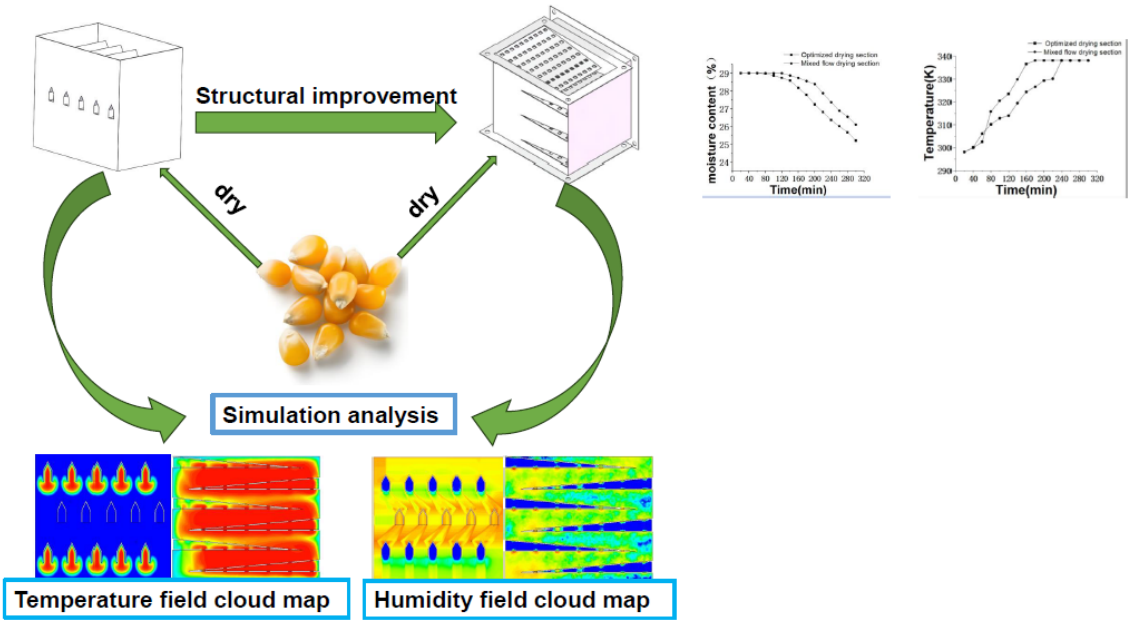

Simulation Analysis of Key Component Structure Optimization of Corn Mixed Flow Drying Device

Siyu Chen, Rui Qiao, Tian Yu, Wanxin Song, and Chunshan Liu *

This study designed a corn kernel drying device and optimized the structure of key components. FLUENT software was used for numerical simulation of wet heat coupling. The differences in physical fields were compared within the drying section before and after optimization. The optimized drying section exhibited improved drying uniformity, drying efficiency, and drying quality. The optimized drying section took 180 seconds for the temperature at the center point to reach the expected value, while the mixed flow drying section took 240 seconds. The moisture content of the optimized drying section decreased to 3.79% at this point, while that of the mixed flow drying section was 2.89%. The results indicated that the drying uniformity and efficiency of the optimized drying structure were higher than those of the mixed flow drying structure. This research provides important data for the design of corn drying equipment.

DOI: 10.15376/biores.20.2.3085-3100

Keywords: Corn; Layered drying; Mixed flow drying; FLUENT wet heat coupling

Contact information: College of Mechanical Engineering Jiamusi University, Jiamusi 154007, China;
** Corresponding author: liuchunshan_2001@163.com*

INTRODUCTION

Corn is one of the most important crops in the food industry, with an annual output of up to one-third of the total grain production, and its planting area is second only to rice and wheat (Cheng *et al*. 2010; Wei 2018). Corn has a very high moisture content after harvesting, and high moisture corn is not suitable for storage. It needs to be lowered to a qualified standard before it can be stored (Ren *et al*. 2024). Therefore, the drying of corn is very important, and different drying device structures, different gas flow directions, and different drying process parameters all have an impact on the drying quality and efficiency of corn kernels (Wang *et al*. 2021; Wei *et al*. 2023).

The application of mixed flow drying is the most widely used. Corn can be heated and dried by three directions of hot air, namely cross flow, co-flow, and counter flow, in the drying section of the mixed flow dryer. Therefore, mixed flow achieves good drying quality and low energy consumption, such that it is widely used (Lv *et al*. 2005). However, during the drying process, the stacking thickness of corn makes mixed flow drying still belong to deep bed drying, which cannot fundamentally solve the drawbacks of deep bed drying. Improving the structure of the mixed flow drying device is crucial for enhancing drying efficiency and uniformity (Jian *et al*. 2022). Compared to mixed flow drying, thin-layer drying has the advantages of high drying efficiency, strong drying uniformity, and good drying quality, and is widely used in various product drying operations (Yang *et al*. 2023).

The drying process is a very complex process, and optimizing its structure through extensive experiments is time-consuming, labor-intensive, and costly (Wang *et al.* 2012). Therefore, researchers are gradually committed to applying computer technology to the study of drying processes. By numerically simulating physical fields such as humidity and temperature fields during the drying process, the drying mechanism of corn kernels is analyzed, and based on this, the drying device is designed and optimized. Some scholars have conducted research on the structure of dryers, used CFD technology to establish mathematical models of the drying process, and improved the drying device based on the results (Pierre-Sylvain 2008). Kjær *et al*. (2018) and Smolka *et al*. (2010) used numerical simulation techniques to simulate and analyze the drying process, studied the changes in various physical fields during the drying process. Based on this, they designed and optimized the drying device to improve its drying quality and efficiency

Recent research mainly has focused on the study and continuous improvement of mixed flow drying structures. There is relatively little research on convenient methods such as layered drying and thin-layer drying. This article designs a corn kernel drying device to address the problems of uneven drying, low drying efficiency, and poor drying quality that is encountered in mixed flow drying devices at present. Based on fluid wet heat coupling simulation, the structure of the drying section is improved, and the advantages of thin-layer drying are utilized to study and analyze the changes in the fluid physical field inside the drying section. A comparative analysis was conducted on the distribution changes of fluid velocity field, temperature field, and humidity field during the drying process of different drying stage structures before and after improvement, aiming to provide technical support for improving the drying efficiency and quality of corn kernel drying devices.

EXPERIMENTAL

This article focused on the drying characteristics of corn kernels and analyzed the differences in heat and mass transfer laws between two different structures in the drying section before and after optimization under the same working conditions. Using Solid Works software to establish a corn kernel drying device model, the drying section model was structurally simplified and the fluid domain was extracted through the Space claim interface in the ANSYS workbench section without changing the drying mechanism. The preliminary design includes two drying sections with external dimensions of 445 × 303 × 410mm; 33.72 kg of grain can be stored in each drying section.

Structural Design of Corb Kernel Drying Device

The corn kernel drying tower consisted of a grain inlet, a storage section, a tempering section, a drying section, a blower, a heat source box, a hoist, a grain outlet, a corner box, *etc*., as shown in Fig. 1. The internal dimensions of the drying tower were 445 × 303 × 1770 mm.

Structure and Optimization of Mixed Flow

There were three rows of angular boxes evenly arranged in the mixed flow drying section, with the first and third rows as air inlets and the second row as exhaust outlets. The width of the corner box was 30 mm, the height was 56 mm, and the spacing between corner boxes was 80 mm. Hot air entered the mixed flow drying section through the air inlet, came into contact with the corn kernels, and dried them, as shown in Fig. 2(a).

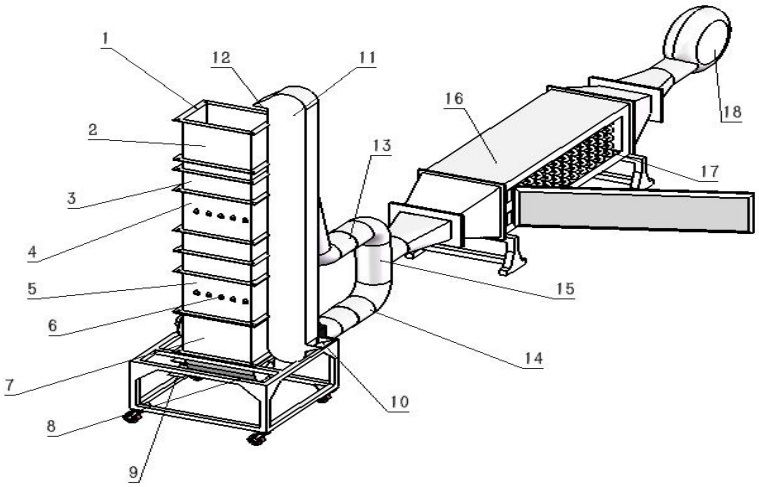

Fig. 1. Drying Device. 1. grain inlet, 2. grain storage section, 3. connecting section, 4. upper drying section, 5. lower drying section, 6.exhaust port, 7.grain discharge section, 8. grain discharge auger, 9. grain outlet, 10. feed inlet, 11. bucket elevator, 12. discharge outlet, 13. upper ventilation duct, 14. lower ventilation duct, 15. control tee, 16. heat source box, 17. electric heating tube, 18. blower

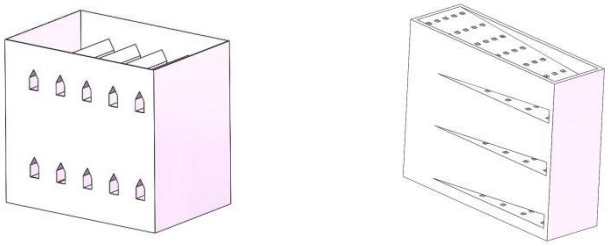

(a).Mixed flow drying section **(b)**.Optimized drying section

Fig. 2. Optimize the structure diagram of the drying section before and after optimization

Figure 2(b) shows the optimized structure of the drying section, with external dimensional parameters consistent with those of the mixed flow drying section. In order to reduce the stacking thickness of corn kernels and improve drying uniformity, six layers of partitions were designed inside it. After experimental verification, it was found that the overall drying effect is optimal when the stacking thickness of corn kernels is 30 mm. In order to ensure the reasonable utilization of the accumulated temperature of corn kernels for the slow drying process, combined with the overall structural dimensions of the drying section designed in this article, when the slope of the partition is 8 °, the average thickness between partitions is 30 mm. At the same time, a certain slope is set for the partition to allow corn kernels to flow smoothly into the lower part of the drying section. This not only reduces the stacking thickness of corn kernels, but it also ensures the rational utilization of accumulated temperature, improving drying quality and efficiency (Zhan 2023).

To ensure that corn kernels could flow smoothly downwards along the partition, the slope of the partition was designed to be 8°. To increase the contact area between hot air and corn kernels, ventilation holes were evenly distributed above and below the partition. Hot air entered the interior of the partition from the side of the partition, and then it entered the drying section through the ventilation holes for drying.

The drying section was made of stainless steel, and the mixed flow drying section was equipped with air filters at the inlet and outlet. The optimized drying section was equipped with air filters outside the partition to avoid grain leakage.

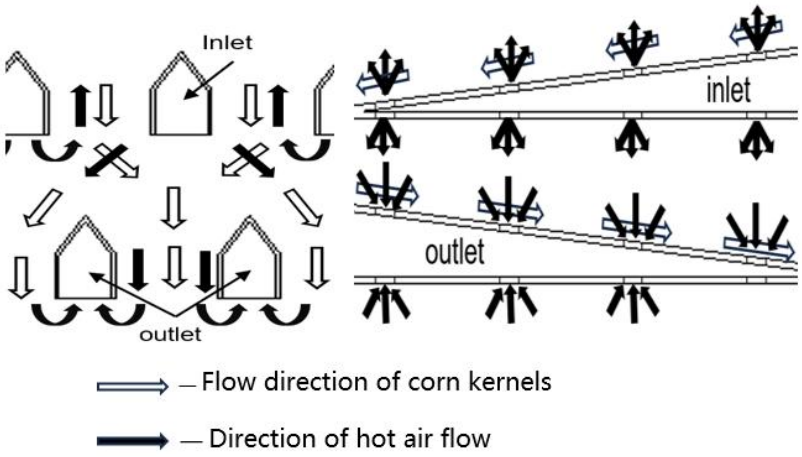

Fig. 3. Drying principle diagram of the drying section before and after optimization

Figure 3 shows the gas flow direction inside the drying section and the flow direction of corn kernels before and after optimization. It could be seen that the structure of the drying section before and after optimization had not changed in the drying form of corn kernels inside. During the drying process, corn kernels could be simultaneously dried by hot air in three directions: parallel flow, cross flow, and counter flow.

Numerical Simulation Mathematical Model

Porous media model

Porous media refers to a complex model composed of irregular solid particles and irregular gaps formed between particles (Seyed Mostafa and Namazi 2019). Corn kernels also had various irregular gaps during the stacking process, so the grain pile was idealized as a porous medium model.

The continuous medium method was generally used to study the accumulation of porous media in corn kernels, treating corn kernels as continuous moist solids without considering the different internal structures of corn kernels (Liu and Yang 2005). The construction of a mathematical model for wet heat transfer in porous media was very complex, involving many aspects such as heat and mass transfer, fluids, strain, and other difficult to define problems. To simplify the calculation of the mathematical model required in this article, the following assumptions were made for porous media (Wang 2014; Mou *et al*. 2015).

1. The stacking of corn kernels in the drying stage is an isotropic porous medium;
2. The shrinkage deformation of corn kernels is ignored;
3. Dry media (such as hot air, water vapor, etc.) are considered ideal gases;
4. No thermal radiation occurs between grains;
5. The gaps formed by stacking corn kernels in the drying section are connected, and the drying medium flows evenly;
6. The heat production of corn kernels themselves is neglected.

Corn kernels followed three conservation laws during the drying process, namely energy conservation, mass conservation, and momentum conservation (Zheng *et al*. 2020). The temperature and humidity control equations were derived for corn kernels and drying media based on the laws of conservation of mass and energy. Any fixed parallelepiped was selected within the porous medium area of corn kernel stacking. This parallelepiped was the microelement used for integration calculation.

Water migration control equation

During the drying of corn kernels, the inflow and outflow of moisture content in the microelements at a certain moment could be roughly divided into: the amount of moisture flowing in and out of the microelements through the drying medium, the amount of moisture evaporated from the interior of the corn kernels into the microelements, and the amount of moisture diffused out of the microelements through the drying medium. By calculating the mass of water flowing in and out per unit time, the equation for the change in moisture content of microelements per unit time could be obtained.

$$\varepsilon\rho_a \frac{\partial Y}{\partial t} + \nabla Y \cdot (\varepsilon\rho_a v) = \nabla \cdot (\varepsilon\rho_a D\nabla Y) + \rho_{pd}(\varepsilon - 1)\frac{\partial M}{\partial t} \quad (1)$$

where ε is the porosity of microelements, ρ_a is the air density, Y is the moisture content in dry medium, v is the velocity of fluid in the x, y, and z directions, D is the components of water diffusion coefficient in three directions, ρ_{pd} is the dry density of corn kernels, and M is the dry basis moisture content of corn kernels.

Heat transfer control equation

The manifestation of energy conservation in the research content of this article was that the increase in heat in a micro element was equal to the same amount of heat transferred from the outside to the micro element. In addition, the continuous medium method was generally used to study the accumulation of porous media in corn kernels, thus obtained the heat transfer control equation applicable to this paper (Meng 2022).

$$\frac{\partial(\rho T)}{\partial t} + div(\rho\vec{\mu}T) = div\left[\frac{k_a}{c_p} \cdot gradT_a\right] + S_T \quad (2)$$

where $\vec{\mu}$ is the Darcy velocity, k_a is the gas thermal conductivity in three directions, T_a is the temperature of drying medium, c_p is the specific heat capacity of drying medium, T is the temperature of corn kernels, and S_T is the dry density of corn kernels.

Momentum conservation equation

The embodiment of momentum conservation in this article was that the rate of change of the momentum of the fluid in the microelements relative to time was equal to the resultant force exerted on the microelements by the external environment (Wang 2016) Due to the conditional assumptions made in the previous section regarding porous media models, only the motion of incompressible viscous fluids was considered here. The momentum conservation equation is shown in Eq. 3 (Guo *et al*. 2012),

$$\frac{D\vec{V}}{D_t} = \vec{f} - \frac{1}{\rho}\nabla p + \frac{\mu}{\rho}\nabla^2\vec{V} + \frac{1}{3}\frac{\mu}{\rho}\nabla\left(\nabla\vec{V}\right) \quad (3)$$

where ρ is the density of microelements, p is the pressure, $\vec{f}$ is the quality power, $\vec{V}$ is the vector velocity, and μ is the dynamic viscosity.

Simulation Model

The object studied in this article was the heat and mass transfer laws of corn kernels during the drying process. Therefore, the extracted fluid domain model was a pure fluid region, and the obtained fluid domain model was imported into the ICEM CFD module for grid partitioning. The quality of the grid affected the accuracy of subsequent simulation

results, so the grid quality must meet the standard. The average grid quality divided in this article was above 0.8, which meets the simulation standards.

Parameter Settings

To conduct numerical simulation calculations, it was necessary to know the physical parameters of corn kernels, including porosity, average density, equivalent diameter, average moisture content, *etc*. Based on these physical parameters, the viscous resistance coefficient and inertial resistance coefficient of porous media could be calculated. The variety of corn kernels was Songyu 438, and its related physical parameters had been measured by experiments conducted within the research group, as shown in Table 1 (Chen *et al*. 2024).

Table 1. Relevant Physical Property Parameters of Corn Kernels

Corn moisture content (%)	28.5
Corn porosity (%)	0.411
Average density of corn (kg/m^{-3})	1213
Equivalent diameter of corn (mm)	7.82
Equivalent diameter of corn ($J \cdot kg^{-1} \cdot K^{-1}$)	2072
Thermal conductivity of corn ($W \cdot m^{-1} \cdot K^{-1}$)	0.1435
Viscous drag coefficient	12256963
Inertial drag coefficient	3797

FLUENT simulation could not achieve wet heat coupling calculation, and users needed to compile and write the moisture migration control equation, energy equation, and momentum conservation equation as UDF files to load into FLUENT software to achieve wet heat coupling simulation. The UDF code is shown in Fig. 4.

```
#include "udf.h"
DEFINE_SOURCE(xmom_source,cell,thread,dS,eqn)
{
    Const real c2 = 100.0;
            .
            .
            .
    Con = c2*0.5*C_R(cell,thread)*x[1];
    Source = -con*fabs(C_U(cell,thread))*C_U(cell,thread);
    dS[eqn] = -2*con*fabs(C_U(cell),thread);
    return source
}
```

Fig. 4. Code diagram of temperature and humidity changes in porous media area

Corn kernel drying was simulated with FLUENT software; the changes in physical fields such as temperature, humidity, and velocity during the drying process were analyzed.

This simulation was a transient simulation, with turbulence model selected as Model k-ε and working environment at standard atmospheric pressure.

The changes in temperature and humidity fields required the participation of source term functions, with a viscous resistance coefficient of 12260000 and an inertial resistance coefficient of 3797. The main directions in the porous medium region were Y=-1 and Z=1. The setting of boundary conditions, with the inlet being the velocity inlet, the inlet wind speed was 0.65 m/s, and the temperature was 338.2 K; The outlet was a pressure outlet, and the outlet temperature was set to 306.2 K; Assuming the outer shell of the drying section was made of insulation material, with a thickness of 0.001 m and a temperature of room temperature of 298.2 K.

The time step for numerical simulation calculation was set to 1/1000, with 300000 time steps and 3000 automatically saved steps. The maximum number of iterations was set to the default value. After the calculation was completed, CFD-post software was used to perform post-processing on the simulation results.

RESULTS AND DISCUSSION

Velocity Field Analysis

Velocity field of mixed flow drying section

Figure 5 shows the steady-state velocity field distribution during the transient calculation process of the mixed flow drying section during hot air drying.

Figures 5(a) and 5(b) show the wind speed at different positions in the drying section under different cross-sections. The closer the color is to red, the higher the wind speed at that location, while the blue area indicates lower wind speed or even no air flow. In Fig. 5(a), the maximum wind speed was 0.65m/s at the air inlet. The hot air entered the corn kernel area through the angular box and was affected by the resistance of the corn kernels. It was distributed in layers along the vertical direction of the angular box at the air inlet and gradually decreased. The farther away from the angular box, the lower the wind speed. As shown in Fig. 5(b), under the action of gravity, the hot air entered the mixed flow drying section along the inlet angular box in a parabolic downward flow. There was almost no hot air distribution in the corn kernel area above the angular box and the edge area of the mixed flow drying section, and the hot air was blocked by the side wall of the angular box, which resulted in turbulence in the corn area and poor uniformity of the hot air.

Figures 5(c) and 5(d) are vector plots of wind speed at two cross-sections. The colors of the arrows in the vector plots also indicate the magnitude of the wind speed, and the density of the arrows indicates the magnitude of the air volume. The hot air entered the drying section from the angled box of the intake pipe and spreads downwards, experienced a significant decrease in velocity due to the viscous and inertial resistance of the corn kernels. The hot air distribution was more concentrated below the intake angle box, flowing through the corn kernels towards the middle exhaust angle box and concentrated below the exhaust port. The closer it was to the exhaust port, the faster the speed.

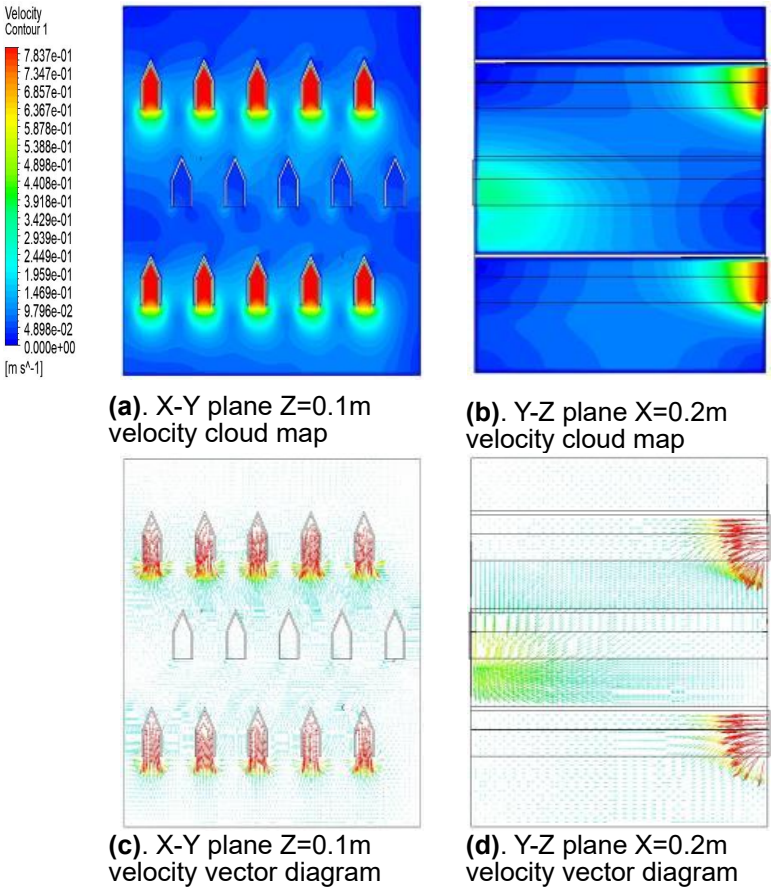

Fig. 5. Distribution of velocity cloud map in mixed flow drying sections

Optimized drying section velocity field

Figure 6 shows the steady-state velocity field distribution during the transient calculation process of hot air drying in the optimized drying section. Figure 6(a) shows that the maximum velocity of hot air inside the air inlet partition was 0.65m/s, and the velocity distribution showed a layered distribution along the air inlet partition towards the corn kernel area and gradually decreased. In addition, the wind speed at the ventilation holes on the partition increased sharply, even exceeding the wind speed inside the partition. This was because, under the premise of constant flow rate, the smaller the flow area of the fluid, the faster the flow velocity. The presence of partitions reduced the thickness of corn kernels stacked, and the viscous and inertial resistance of the corn area to hot air decreased. Therefore, there was almost no area without airflow distribution in the entire drying section, and the uniformity was greatly improved.

Figure 6 (b) shows the flow direction and diffusion pattern of hot air in the optimized drying section. The hot air entered the corn area through the ventilation holes on the air inlet partition, and began to spread to both sides of the drying section. The airflow flowing out from the ventilation holes above the air inlet partition was denser than that from the ventilation holes below. Due to the large area of the partition, the contact area between the hot air and the corn kernels was increased, and the presence of the partition transforms the originally deep bed drying in the drying section into thin layer drying. The hot air could more easily penetrate the corn area, thus greatly improving the distribution and diffusion uniformity of the hot air in the drying section.

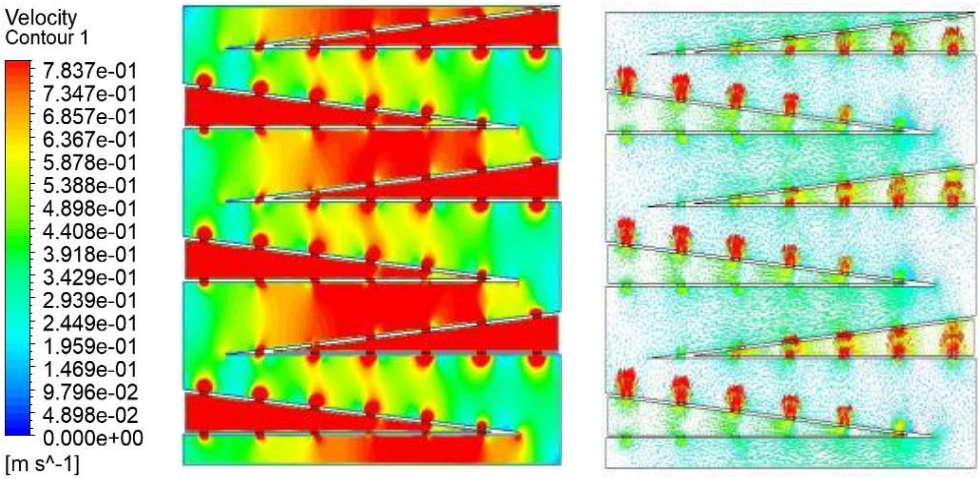

(a).X-Y plane Z=0.2m velocity cloud map

(b).X-Y plane Z=0.2m velocity vector diagram

Fig. 6. Distribution of velocity field in layered drying section

Temperature Field Analysis

To examine the effects of optimizing the two types of drying section structures on drying quality and efficiency, it was necessary to analyze the temperature changes in the simulation results. The time steps and time steps set in the simulation were calculated based on an actual drying time of 300 seconds.

Analysis of Temperature Field in Mixed Flow Drying Section

Figure 7 shows the temperature distribution cloud map of the mixed flow drying section on the horizontal characteristic interface (X-Z plane Y=0.1m) and the vertical characteristic interface (X-Y plane Z=0.2m). The time step and number of time steps set during the simulation calculation correspond to the actual hot air-drying time of 300 seconds. The calculation results would be saved every 3 seconds. Four sets of simulation results were selected with drying times of 75s, 150s, 225s, and 300s for analysis.

As shown in Figs. 7(a) to (d), the temperature inside the intake angle box was higher than that in the corn area, at 338.2 K. As the drying time increased, the hot air began to spread along the corner box below. After flowing into the corn kernel area, the hot air continuously transferred heat to the corn, and the heat of the hot air was continuously lost, showing a layered distribution and gradually decreasing trend. The temperature of the corn kernels in direct contact with the lower end of the intake angle box was significantly higher than in other areas. The side walls of the angle box were in direct contact with the corn kernels, and heat was transferred through the side walls. Therefore, the temperature near the side walls inside the angle box decreased to a certain extent.

As shown in Figs. 7(e) to (h), in the horizontal feature interface, the speed of temperature diffusion in the intake direction was higher than on both sides. Due to the characteristics of the mixed flow drying section, the stacking thickness of the corn area was relatively thick, and the response speed to temperature changes was slow. After 300 seconds of drying, there was still a large area of corn area without temperature changes, resulting in low drying efficiency.

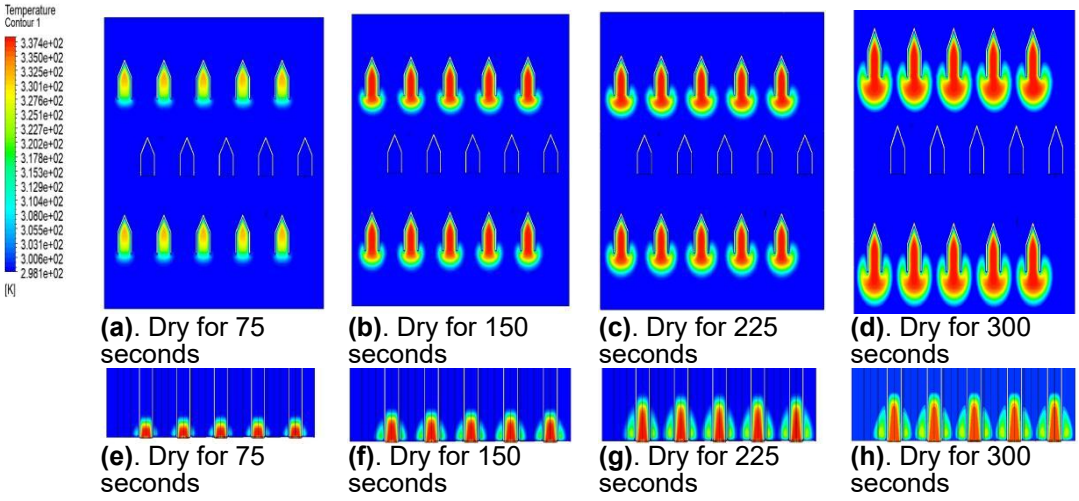

Fig. 7. Temperature distribution cloud map of mixed flow drying section at different drying times. Note: a, b, c, and d are vertical feature interfaces (Y-Z plane X=0.2m); e. f, g, h are horizontal feature interfaces (X-Y plane Z=0.1m)

Analysis of Temperature Field in Optimized Drying Section

Figure 8 shows the temperature field distribution over time during the transient calculation process of hot air drying for 300 seconds on the horizontal characteristic interface (X-Z plane Y=0.1m) of the optimized drying section.

As shown in Fig. 8(a), the temperature inside the air inlet partition was highest at 338.2 K during the initial drying stage. The hot air entered the corn kernel area through the ventilation holes on the partition, continuously transferring heat with the corn kernels. Therefore, the temperature in the corn kernel area was also constantly increasing. The temperature outside the partition showed a layered diffusion trend at the location of the ventilation holes, and the further away from the ventilation holes, the lower the temperature.

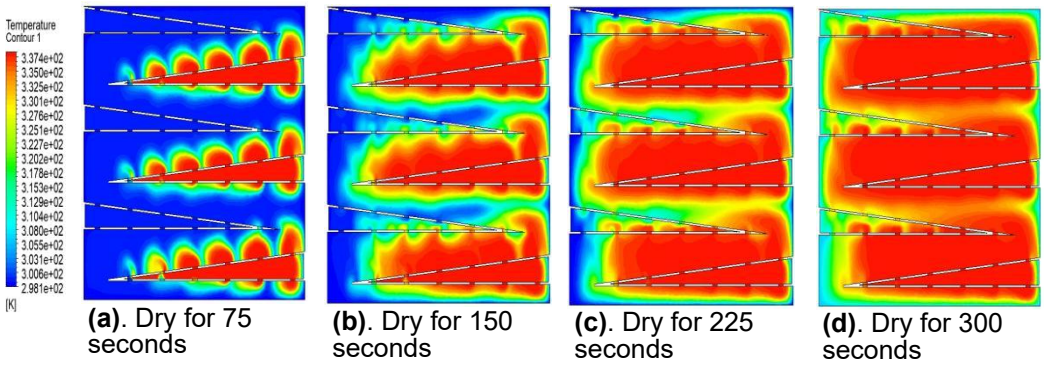

Fig. 8. Cloud map of temperature distribution in the drying section optimized for different drying times

In Fig. 8(b), due to the triangular shape of the partition and the connection of the drying section shell on the right side, the space on the right side was larger than that on the left side of the partition. Therefore, the temperature inside the drying section showed a trend of continuously spreading from the right side to the left side, and the temperature of the corn kernel area in contact with the partition was significantly higher than that of other

corn kernel areas. From Figs. 8(c) and (d), with the continuous flow of hot air, almost all of the corn kernel areas in the drying section had reached the expected drying temperature, and the hot air passed through the corn kernel areas and flowed into the exhaust partition through ventilation holes.

The presence of partitions reduced the stacking thickness of the corn kernel area and shifted the drying mode to thin-layer drying. Therefore, the optimized drying section of the corn kernel area responded very quickly to temperature changes. In addition, compared with the angular box, the area of the partition increases, and the contact area between the hot air and the corn kernels also increased accordingly. It could be seen that the optimized drying section has significantly better uniformity of temperature distribution and diffusion rated than the original mixed flow drying section.

Humidity Field Analysis

Analysis of humidity field in mixed flow drying section

Figure 9 shows the humidity field distribution over time during the transient calculation process of hot air drying for 300 seconds on the vertical characteristic interface (X-Y plane Z=0.2m) of the mixed flow drying section.

Figure 9(a) shows that at a drying time of 75 seconds, there was almost no change in humidity in the corn kernel area within the drying section, and only the moisture content inside the air inlet began to decrease. As the drying time increased, hot air began to flow and spread, and the moisture content in the corn kernel area below the inlet angle box began to decrease. The closer it was to the bottom of the angle box, the better the drying effect. This distribution characteristic was consistent with the changes in temperature and wind speed. The moisture contented changes in the corn kernel area shown in Figs. 9(c) and (d) were still concentrated near the corner box, while the corn kernel areas above the drying section and near the exhaust corner box had only small moisture content changes and no concentrated areas. This phenomenon was determined by the characteristics of wind speed distribution in the drying section. The characteristics of deep drying determine that the area with the fastest humidity changed in mixed flow drying was definitely below the inlet angle box. However, the drying effected above and at the edges of the inlet angle box in the mixed flow drying section was not good, and the uniformity was poor.

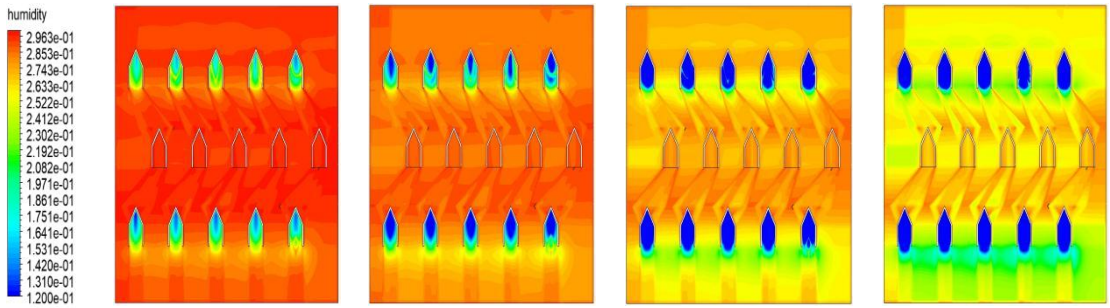

(a).Dry for 75 seconds **(b)**.Dry for 150 seconds **(c)**.Dry for 225 seconds **(d)**.Dry for 300 seconds

Fig. 9. Humidity distribution cloud map of mixed flow drying section at different drying times

Analysis of humidity field in the optimized drying section

Figure 10 shows the humidity field distribution over time during the transient calculation process of hot air drying for 300 seconds on the vertical characteristic interface (X-Y plane Z=0.2m) of the optimized drying section.

In Fig. 10(a), the location where the moisture content first changes was inside the partition between the inlet and outlet, which was also the location where the moisture migration rate, changed the fastest in the early stage of drying.

In Fig. 10(b), as the drying time increased, hot air diffused from the ventilation holes on the air inlet partition to the corn kernel area. The water vapor evaporated from the internal moisture of the corn kernel entered the hot air under the action of temperature and pressure differences, and the moisture contented of the corn kernel area began to decrease.

In Fig. 10(c), the moisture content in the corn kernel area near the air inlet partition changed significantly and showed a trend of spreading from the right to the left, which was determined by the shape of the partition.

In Fig. 10(d), there was a significant change in the moisture content of most corn kernel areas, with the highest decrease in moisture content observed in the corn kernel areas above and below the air inlet partition. However, a small portion of the area near the ventilation holes on the exhaust partition still had a high moisture content. This was because the moisture in the corn kernel area flowed towards the exhaust port after entering the hot air, and when it entered the partition through the ventilation holes, it would concentrate near the ventilation holes, which would increase the moisture content to a certain extent. But overall, the uniformity of water contented changes in the optimized drying section was very high.

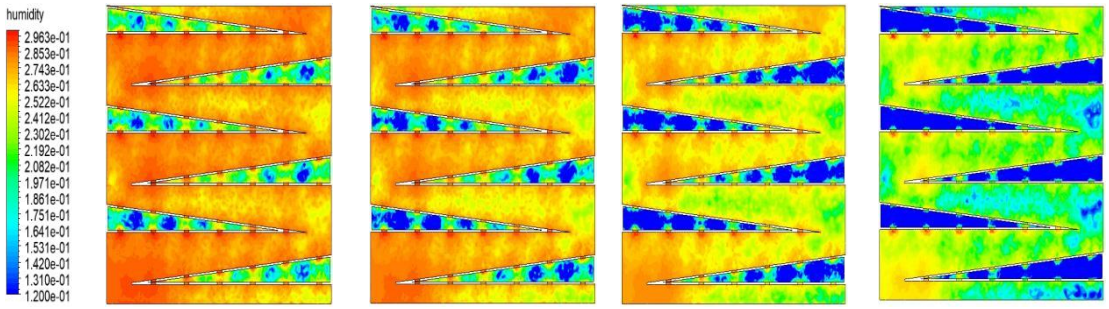

(a). Dry for 75 seconds **(b)**. Dry for 150 seconds **(c)**. Dry for 225 seconds **(d)**. Dry for 300 seconds

Fig. 10. Cloud map of humidity distribution in the drying section optimized for different drying times

Comparative Experiment of Drying Sections with Different Structures

The selected experimental object for this experiment was the corn kernel of variety Songyu 438. The initial moisture content was 29%. The procedure was to spread the harvested corn kernels evenly in the drying section before and after optimization. The drying section test bench was made of stainless steel material, connected to the heat source box and blower on the side, and equipped with air filters at the inlet and outlet to prevent grain leakage. The relevant experimental parameters selected for this experiment were consistent with the parameters set for numerical simulation calculations.

The data during the experiment were recorded and organized into a table. The obtained data results were processed using Origin software, as shown in Fig. 11.

Figure 11(a) shows the temperature variation curves at the center point of the drying section for two different drying modes. It could be seen that the optimized drying section had a significantly higher rate of temperature rise at this point than the original mixed flow drying section, and the time required to reach the expected drying temperature of 338.2 K at this point was also less than that of the mixed flow drying section. This was because layered drying fundamentally transformed the deep bed drying mode, reduced the stacking thickness of corn kernels, and decreased the viscous and inertial resistance to hot air, making it easier for hot air to pass through the corn area after entering the drying section through the air inlet. Compared to mixed flow drying mode, the response to temperature changes became more rapid, improving drying efficiency.

Figure 11(b) shows the moisture content variation curves at the center point of the drying section for two different drying modes. Firstly, it could be seen that within the selected drying time of 300 seconds, the moisture content of the drying section before and after optimization did not change significantly at this point. After optimization, the moisture content of the drying section at this point decreased by about 3.79%, while the moisture content of the original mixed flow drying section only decreased by 2.89% at this point. The moisture content of both drying modes did not change during the initial stage of the experiment, but compared to the original mixed flow drying section, the moisture content change in the optimized drying section started earlier, and within the same drying time, the moisture content of corn kernels at that point in the optimized drying section decreased faster than in the mixed flow drying section.

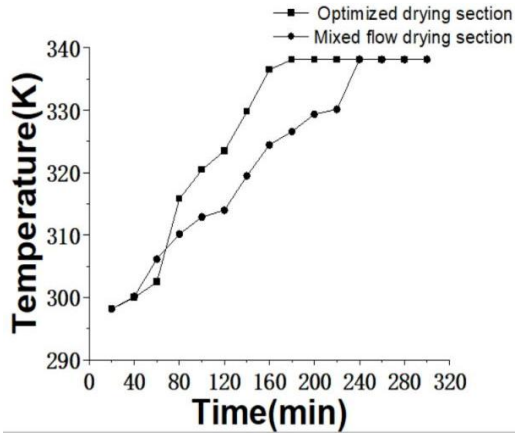

(a). Temperature change curve at point M

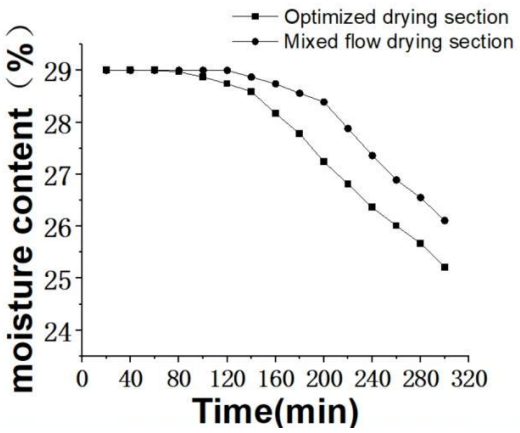

(b). Curve of moisture content change at point M

Fig. 11. Variation pattern of drying characteristics at point M in the drying section

The experimental results showed that both the response speed to temperature changes and the moisture content changes at this point were better in the optimized drying section than in the mixed flow drying section. Therefore, it could be concluded that the optimized drying section achieved significant improvements in drying efficiency and uniformity compared to the original mixed flow drying section.

CONCLUSIONS

1. The optimized drying section structure was superior to mixed flow drying in terms of the uniformity and efficiency of hot air flow. The optimized drying method reduced the stacking thickness of corn kernels, reducing the resistance of hot air penetrating the corn area and making it easier to reach other positions within the drying section. Compared to mixed flow drying, the dead corners of the drying section were significantly reduced.
2. The temperature change rate in the optimized drying section was significantly faster than that in the original mixed flow drying section. Only nearly half of the corn areas in the mixed flow drying section reached the specified drying temperature within 300 seconds of drying, while almost all the corn kernel areas in the optimized drying section reached the expected drying temperature of 338.2 K. Compared to the original mixed flow drying, the optimized drying section structure significantly improves the response speed to changes in hot air temperature.
3. The moisture content changes in the mixed flow drying section during the 300 s drying time were concentrated below the inlet angular box. The area of corn with moisture content changes was not large, and the decrease in moisture content in this area was also relatively small, with an average decrease of only about 1.5%. The optimized drying section, with its internal partitions, reduced the stacking thickness of corn kernels, allowed hot air to flow faster in the corn kernel area. In addition, compared to the angular box, the ventilation holes on the partition increased the area of contact between hot air and corn kernels, improve drying efficiency, and increase the rate of moisture content change.
4. In the comparative experiment of two drying modes, the optimized drying section showed better temperature changes and moisture content reduction rate at the selected center point position than the original mixed flow drying section. Within the same drying time, the mixed flow drying section took 240 seconds to raise the temperature to the expected value at this point, while the optimized drying section only took 180 seconds. In terms of moisture content changes, the moisture content of corn kernels at the center point of the original mixed flow drying section decreased by 2.89%, while the optimized drying section reduced the moisture content of corn kernels at this point by 3.79%

ACKNOWLEDGMENTS

This research was supported by the Joint Guidance Project of Heilongjiang Provincial Natural Science Foundation (LH2023C059), the National Foundation Cultivation Project of Jiamusi University (JMSUGPZR2023-014), Jiamusi Science and Technology Plan Innovation Incentive Project (NY2023JL0007), 2023 Higher Education Research Project of Heilongjiang Higher Education Association (23GJYBF091) and the Education Teaching Reform Research Project of Jiamusi University (2023JY6-41).

REFERENCES CITED

Chen, S. Y., Wang, Z. X., Wu, W. F. *et al*. (2024). "Simulation analysis of circulation ventilation and longitudinal ventilation in corn storage silos based on EDEM Fluent," *Journal of Agricultural Engineering* 40(06), 40-49. DOI: 10.11975/j.issn.1002-6819.202310157

Chen, Z. J. (2019). *Numerical Analysis and Structural Optimization of the Flow Field Inside the Corn Co current Drying Oven*, Master's Thesis, Heilongjiang Bayi Agricultural Reclamation University.

Cheng, J. H., Zhou, X. Q., Zhang, Y. R. Deng, L. Z., and Ren, H. L. (2010). "Correlation analysis between quality characteristics of dry corn and starch yield," *Journal of Henan University of Technology (Natural Science Edition)* 31(04), 37-42. DOI: 10.16433/j.cnki.issn1673-2383.2010.04.016

Gong, Z. L., Chen, C. H., Tao, Y. F., and Guo, H. X. (2021). "Simulation study on temperature uniformity of oil tea seed mesh belt dryer," *Agricultural Mechanization Research* 43 (06), 42-46. DOI: 10.13427/j.cnki.njyi.2021.06.008

Guo, J. (2012). *Optimization Study on Transfer Parameters of Wet Heat Model for Grain Pile*, Master's Thesis , Henan University of Technology, China.

Kjær, L. S., Poulsen, M., Sørensen, K., and Condra, T. (2018). "Modelling of hot air chamber designs of a continuous flow grain dryer," *Engineering Science and Technology* 21(5), 1047-1055. DOI: 10.1016/j.jestch.2018.02.002

Liu, X. D., and Yang, B. B. (2005). "Review and prospect of porous media drying theory," *Journal of China Agricultural University* (04), 81-92.

Lv, X. R. (2005). *Theoretical and Experimental Study on Intelligent Control of Grain Drying Process*, Master's Thesis , Northeastern University, Shenyang City, Liaoning Province

Meng, F. (2022). *Numerical Simulation and Experimental Study on Moisture and Heat Transfer during Corn Drying Process*, Master's Thesis, Henan University of Technology, Zhengzhou City, Henan Province.

Mou, G. L., Zhang, X. J., and Shi, Z. L. (2015). "Research on improved design of circulating drying machine combined with fluent simulation software," *Zhejiang Agricultural Journal* 27(04), 684-689. DOI: 10.3969/j.issn.1004-1524.2015.04.29

Pierre-Sylvain, M. (2008). "Computational fluid dynamics (CFD) modelling applied to the ripening of fermented food products: Basics and advances," *Trends in Food Science & Technology* 19, 472-481. DOI: 10.1016/j.tifs.2008.01.014

Ren, L., Zheng, Z., Fu, H., Yang, P., Xu, J., and Yang, D. (2024). "Hot air–assisted radio frequency drying of corn kernels: the effect on structure and functionality properties of corn starch," *International Journal of Biological Macromolecules* 267, article 131470. DOI: 10.1016/j.ijbiomac.2024.131470

Seyed, M. H., and Namazi, M. (2019). "Pore-scale numerical study of flow and conduction heat transfer in fibrous porous media," *Journal of Mechanical Science and Technology* 33, 2307-2317. DOI: 10.1007/s12206-018-1231-4

Smolka, J., Nowak, A. J., and Rybarz, D. (2010). "Improved 3-D temperature uniformity in a laboratory drying oven based on experimentally validated CFD computations," *Journal of Food Engineering* 97, 373-383. DOI: 10.1016/j.jfoodeng.2009.10.032

Wang, D. Y., Wang, J., Qiu, S., Zhan, T. Y., Tao, D. B., and Zhang, B. H. (2021). "Optimization and experiment of parameters for rice hot air drying and slow drying process," *Journal of Agricultural Engineering* 37(17), 285-292. DOI:

10.11975/j.issn.1002-6819.2021.17.033
Wang, W. Y. (2016). "Method and device for measuring convective heat and mass transfer coefficient during the drying and ventilation process of grain piles," *Beijing University of Posts and Telecommunications*.
Wang, Y. C., Zhang, Z. J., Wu, Z. D., Ding, D. Q., and Wang, S. F. (2012). "Application of computational fluid dynamics technology in grain storage," *Chinese Journal of Grain and Oil* 27(05), 86-91.
Wang, Z. H. (2014). *Numerical Simulation and Experimental Study on the Heat and Moisture Transfer Process of Stored Grain Piles*, Ph.D. Dissertation, China Agricultural University, Beijing City.
Wei, Y. F. (2018). *Application of Corn Drying Heat Pump Technology and Optimization Design of Drying Tower Corner Box*, Master's Thesis , Henan University of Technology, Zhengzhou City, Henan Province.
Wei, Z., Pan, T. T., Li, J. J., Zhao, J. L., and Zhai, A. H. (2023). "The effect of different rice drying methods on the quality of rice before and after soaking," *Food Industry Technology* 1-14. DOI: 10.13386/j.issn1002-0306.2023030229
Yang, M. J., Liu, E. G., Wu, Y. F., Yang, S., Yang, L., Pu, Y. J., Zhao, L. J., and Song, W. D. (2023). "Development and testing of an online moisture content measurement device for thin layer hot air drying process," *Journal of Agricultural Engineering* 39(04), 47-56. DOI: 10.11975/j.issn.1002-6819.202211176
Yan, J C., Wei, H., You, Z. Y., Wu, H. C., Xu, X. W., and Xie, H. X. (2023). "Energetic and exergetic performances during drying of freshly harvested peanut with industrial mixed-flow dryer," *Energy Reports* 8, 7457-7467. DOI: 10.1016/j.egyr.2022.05.252
Zhan, T. Y. (2023). *Experimental Study on Optimization of Deep Bed Slow Drying Process for Rice*, Master's Thesis , Shenyang Agricultural University, Shenyang City, Liaoning Province.
Zheng, X. Z., Liu, H., Shen, L. Y., Wang, J. W., Wang, L., Zhu, Y., *et al*. (2020). "Research on temperature controlled hot air drying process of rice based on glass transition," *Journal of Agricultural Machinery* 51(01), 331-340. DOI: 10.6041/j.issn.1000-1298.2020.01.036

Article submitted: November 6, 2024: Peer review completed: January 18, 2025; Revised version received: February 21, 2025; Accepted: February 23, 2025; Published: March 5, 2025.
DOI: 10.15376/biores.20.2.3085-3100